Greenhouse gas production, diffusion and consumption in a soil profile under maize and wheat production

Erik S. Button [a], Miles Marshall [a], Antonio R. Sánchez-Rodríguez [b], Aimeric Blaud [c], Maïder Abadie [d], David R. Chadwick [a], David L. Jones [a,e,*]

[a] School of Natural Sciences, Bangor University, Bangor LL57 2UW, UK
[b] Departamento de Agronomía, Universidad de Córdoba, Córdoba 14071, España
[c] School of Applied Sciences, Edinburgh Napier University, Sighthill Campus, Edinburgh EH11 4BN, UK
[d] Sustainable Agriculture Sciences Department, Rothamsted Research, Harpenden AL5 2JQ, Hertfordshire, UK
[e] SoilsWest, Centre for Sustainable Farming Systems, Food Futures Institute, Murdoch University, 90 South Street, Murdoch, WA 6105, Australia

ARTICLE INFO

ABSTRACT

Agricultural soil emissions are a balance between sinks and sources of greenhouse gases (GHGs). The fluxes of GHGs from soils are complex and spatially and temporally heterogeneous. While the soil surface is the exchange site with the atmosphere and is commonly where GHG fluxes are measured, it is important to consider processes occurring throughout the soil profile. To reduce emissions and improve agricultural sustainability we need to better understand the drivers and dynamics (production, consumption, diffusion) of these gases within the soil profile. Due to the heterogeneous nature of GHG processes at small to large scales, it is important to test how these processes differ with depth in different systems. In this study, we measured *in situ* CO_2, N_2O and CH_4 concentration gradients as a function of soil depth over subsequent maize and wheat growing seasons with active gas samplers inserted into an arable field at 10, 20, 30 and 50 cm depths. We found N_2O and CH_4 concentrations increased with depth, but only CO_2 concentrations differed with depth between growing seasons due likely to differences in soil diffusivity driven by soil conditions. Using the concentration gradient method (GM), the CO_2 fluxes at each depth and their contribution to the surface flux were calculated and validated against a chamber method (CM) measured surface flux. We found the GM estimated surface CO_2 flux was only 6 % different in the wheat, but 28 % lower than the surface measured flux in the maize growing season, due to drought conditions reducing the accuracy of the GM. Finally, we measured fluxes of CO_2, N_2O and CH_4 in ambient and highly concentrated headspaces in laboratory mesocosms over a 72 h incubation period. We provide evidence of depth dependent CH_4 oxidation and N_2O consumption and possibly CO_2 fixation. In conclusion, our study provides valuable information on the applicability of the GM and further evidence of the GHG production, consumption and diffusion mechanisms that occur deeper in the soil in a temperate arable context.

1. Introduction

Agricultural soils represent significant sources of CO_2, CH_4 and N_2O to the atmosphere. However, they can also act as greenhouse gas (GHG) sinks (Chapuis-Lardy et al., 2007; Johnston et al., 2009). Net emissions of GHGs from the soil are therefore a balance between production and consumption processes that occur simultaneously in soil. As the pool of soil organic matter (SOM), the principal soil sink of CO_2, grows or shrinks, the potential for microbial decomposition and the resulting net CO_2 flux increases or decreases (Johnston et al., 2009). The net soil-atmosphere flux of N_2O, on the other hand, is dynamically governed by the availability of N, soil conditions and the soil microbial processes that underpin the production and consumption of N_2O in the soil (Chapuis-Lardy et al., 2007). Finally, the CH_4 flux depends almost entirely on O_2 availability when C is not limiting and the temperature is not too low (<0 °C; Le Mer and Roger, 2001). The fluxes of these important agricultural GHGs are complex and spatially and temporally heterogenous, but to improve agricultural sustainability through reduction of GHG emissions, the drivers and dynamics need to be better understood.

---

* Corresponding author at: School of Natural Sciences, Bangor University, Gwynedd LL57 2UW, UK.
  E-mail address: d.jones@bangor.ac.uk (D.L. Jones).

Quantifying the differences between surface and soil profile fluxes and their drivers is important as agricultural practices (e.g. tillage, nitrogen inputs, organic matter amendments, cropping) influence and drive GHG production throughout the soil. While we have a good understanding of soil-to-air GHG fluxes from surface measurements (e.g. closed chamber and eddy-covariance methods; Dossa et al., 2015; Kusa et al., 2008), these do not capture information concerning GHG-related processes occurring deeper in the soil (Wang et al., 2018). In addition, they largely assume that the emissions of GHGs are instantaneous and disregard the possibility of changes in the C and N pools in the soil (Wang et al., 2018). Finally, the soil-to-air flux is not necessarily representative of GHG fluxes in the whole soil profile (Boon et al., 2014; Clark et al., 2001). To capture more information on GHG processes that lead to the surface-atmosphere flux, different methods are required.

The concentration gradient method (GM) is an approach that uses the soil profile gas concentration gradient to estimate soil fluxes, which are difficult to measure *in situ*, and extrapolates from this gradient to determine the surface flux. The GM contributes to greater understanding of GHG dynamics at different soil depths, which is essential to better predict movements of C and N in ecosystems (Maier and Schack-Kirchner, 2014). This is especially important in the light of climate change and the increasing interest (e.g. '4 per 1000' initiative) and urgent need for sequestering C in soil and subsoil. The method requires concentration gradient data which we aimed to produce for CO_2, CH_4 and N_2O, which only a few studies have done simultaneously (Wang et al., 2018) and fewer still across different crops (Wang et al., 2013). Typically, concentrations of N_2O and CO_2 in the soil profile are much greater than in the overlying air, while an opposite trend is often found for CH_4 in oxic soils (Wang et al., 2013; Li and Kelliher, 2005; Maier and Schack-Kirchner, 2014; Wang et al., 2018; Xiao et al., 2015). In addition, the presence and characteristics of plant roots can influence GHG concentrations with depth, by stimulating the microbial community with C inputs and enhancing the transport of solutes and gases in the soil profile (Button et al., 2022). However, how soil GHG concentration profiles may differ across multiple soils, climates and crop rotations is poorly studied.

For the utility of the GM in furthering the understanding of the GHG dynamics to be realised, the estimated fluxes need to be reliable. As the performance of the GM is influenced by many factors, including the target GHG, sampling frequency and the method for determining the diffusion coefficient (D_s), it is important to test the limits and opportunities of the method for determining the most effective use of the method (Maier and Schack-Kirchner, 2014). An aim of this study was to test the performance of the GM in estimating CO_2 fluxes across multiple growing seasons and crop rotations at low temporal resolution with a measured D_s against a surface chamber method.

While it is well documented that GHG fluxes differ with depth (Davidson et al., 2004; Wang et al., 2013; Wang et al., 2018), the net GHG flux is a result of a balance between consumption and production processes. For CO_2, CH_4 and N_2O, the consumption process is known as dark CO_2 fixation (Akinyede et al., 2020); methanotrophy (i.e. CH_4 oxidation; Le Mer and Roger, 2001); and N_2O consumption (i.e. complete denitrification) (Maier and Schack-Kirchner, 2014; Neftel et al., 2007), respectively. While these processes have been measured in different systems, how their fluxes differ with depth is not fully understood. A further aim of this study was to quantify GHG consumption fluxes, with an expectation that consumption of GHGs would be depth dependent as consuming microbes and the conditions that support these processes differ with soil depth.

In this study, we measured *in situ* CO_2, N_2O and CH_4 concentration gradients from 10 to 50 cm over a maize and a subsequent wheat growing season. We hypothesised that maize and wheat crops would result in measurable differences in GHG concentration profiles due to their differing rooting characteristics. We also hypothesised that the GM would be a reliable method in the estimation of CO_2 fluxes despite low temporal resolution, different growing seasons and crops. To address the

hypothesis that production and consumption of GHGs is depth dependent, a laboratory soil incubation study was also undertaken to measure net production and consumption of CO_2, N_2O and CH_4 in soil taken from different soil depths under different concentrated headspaces.

2. Materials and methods

2.1. Experimental site and soil characterisation

The study site was a lowland (<10 m.a.s.L.) arable field located at the Henfaes Research Centre, Abergwyngregyn, North Wales (53°14′29″N, 4°01′15″W). The site has a temperate oceanic climate regime with long term (>10 y) mean annual temperature of 10.8 °C and annual rainfall of 1066 mm y^{-1}. The field was drilled with forage maize (*Zea mays* L., cv. Emmerson) on the 6th of May 2018 and sown with winter wheat (*Triticum aestivum* L., Mulika) on the 26th of March 2019. The freely draining sandy clay loam textured soil is classified as a Eutric Cambisol (WRB) or Typic Hapludalf (US Soil Taxonomy; Soil Survey Staff, 2014). The field received no N fertilizer in 2018 as the soil mineral N content was already high (34 ± 0.1 mg N kg^{-1} soil, n = 8), but received 2 rates of N fertilizer as ammonium nitrate in 2019: High (150 kg ha^{-1}) and Medium (75 kg ha^{-1}). Plots were established within a randomised block design with 4 blocks and 3 treatment plots per block. The plots receiving Medium and High fertilizer rates both received 40 kg ha^{-1} of N fertilizer on the 7th May, and then a further 35 or 110 kg ha^{-1} on the 30th of May 2019, respectively. The soil was conventionally ploughed both years to a depth of 30 cm at the beginning of the growing seasons in March. As the soil was undisturbed thereafter for >2 months before the first gas samples were taken, the soil was considered to have settled. This is supported by Fiedler et al. (2015) who found soil respiration to return to pre-tillage levels 36 d after tillage.

In 2018, soil from the same field was characterised extensively for chemical, biological and physical properties (mean values presented in Table 1). Soil samples were taken from 4 independent soil pits located ca. 50 m apart at 10 cm depth intervals to a depth of 100 cm and sieved to 5 mm. Soil texture was measured with a LS 13,320 laser diffraction particle size analyser (Beckman-Coulter Inc., Indianapolis, IN). Soil pH and electrical conductivity (EC) were measured in a fresh soil 1:2.5 (w/v) distilled water suspension with a Model 209 pH meter (Hanna Instruments ltd., Leighton Buzzard, UK) and a Jenway 4520 conductivity meter (Cole-Palmer ltd., Stone, UK), respectively. Cation exchange capacity (CEC) was determined using the sodium acetate method of Sumner and Miller (1996). Total soil C and N were determined with a TruSpec® CN analyser (Leco Corp., St Joseph, MI). Soil subsamples (5 g) were extracted with 0.5 M K_2SO_4 (1:5 w/v; 150 rev min^{-1}, 30 min) and the supernatant recovered after centrifugation (14,000 g, 10 min). NH_4^+ and NO_3^- concentrations were determined colorimetrically according to Mulvaney (1996) and Miranda et al. (2001), respectively, on a Power-Wave XS Microplate Spectrophotometer (BioTek Instruments Inc., Winooski, VT, USA). Dissolved organic C (DOC) in the extracts was measured with a Multi N/C 2100/2100 analyser (AnalytikJena AG, Jena, Germany). Soil microbial biomass C (MBC) was measured using the $CHCl_3$ fumigation-K_2SO_4 extraction procedure of De-Polli et al. (2007) using a K_{EC} extraction efficiency values of 0.45 (Vance et al., 1987). Immediately after soil collection, field-moist soil samples (25 g) were sieved (2 mm), frozen (-20 °C), freeze-dried and phospholipid-derived fatty acids (PLFA) were determined according to Bartelt-Ryser et al. (2005). Finally, quantitative PCR (qPCR) analyses of N cycling gene abundance (*nirK*, *nirS*, *nosZ*) were processed at the same time following the methods described in de Sosa et al. (2018).

2.2. Environmental and crop measurements

Rainfall, atmospheric pressure, air and soil temperature and soil volumetric water content (θ) were recorded hourly at a weather station located 50 m from the research site. θ and soil temperature were

Table 1

Physical, chemical and biological soil properties at different depths and root properties from the maize and wheat plots in 2018 and 2019. Where appropriate, the data are expressed on a soil dry weight basis. Values are means ± SEM. Unless stated otherwise, $n = 4$.

Properties		Soil depth (cm)				
		0–10	10–20	20–30	30–40	40–50
Sand (%)		62.9 ± 0.7	62.0 ± 1.3	60.3 ± 2.3	60.3 ± 3.3	62.4 ± 4.4
Silt (%)		16.2 ± 1.3	17.8 ± 0.6	17.8 ± 1.2	17.5 ± 1.5	17.1 ± 1.8
Clay (%)		20.9 ± 1.0	20.2 ± 0.9	21.9 ± 1.5	22.2 ± 2.3	20.6 ± 2.6
Dry bulk density (g cm^{-3})		1.4 ± 0.03	1.4 ± 0.07	1.7 ± 0.1	1.7 ± 0.2	1.8 ± 0.1
Porosity (%)		66 ± 2.0	69 ± 1.1	67 ± 1.0	63 ± 1.2	59 ± 1.8
pH (1:2.5)		6.0 ± 0.1	6.2 ± 0.1	6.5 ± 0.1	6.6 ± 0.1	6.7 ± 0.1
EC (1:2.5 µS cm^{-1})		33 ± 4	32 ± 2	24 ± 1	25 ± 3	19 ± 1
DOC (mg C kg^{-1})		82.3 ± 4	76.8 ± 4	57.0 ± 7	52.0 ± 10	47.1 ± 9
CEC (cmol$_+$ kg^{-1})		14.8 ± 0.2	15.6 ± 0.4	12.7 ± 1.0	12.7 ± 0.5	11.1 ± 1.7
NH$_4^+$ (mg kg^{-1})		2.4 ± 0.1	1.9 ± 0.2	1.7 ± 0.1	1.6 ± 0.1	1.6 ± 0.2
NO$_3^-$ (mg kg^{-1})		10.8 ± 0.7	11.6 ± 2	4.9 ± 0.4	3.3 ± 0.2	2.0 ± 0.1
Total PLFA biomass (nmol g^{-1})		132 ± 9	116 ± 4	58 ± 5	34 ± 3	23 ± 2
nirK gene (x10^8 copies g^{-1})		4.8 ± 0.4	4.5 ± 0.3	2.3 ± 0.3	1.1 ± 0.1	0.7 ± 0.08
nirS gene (x10^6 copies g^{-1})		6.9 ± 0.7	4.9 ± 0.5	1.6 ± 0.4	0.6 ± 0.1	0.2 ± 0.04
nosZ gene (x10^7 copies g^{-1})		5.3 ± 0.3	4.2 ± 0.4	1.3 ± 0.2	0.4 ± 0.07	0.2 ± 0.05
Root density	Maize*	5.4 ± 1.1	0.15 ± 0.02	0.2 ± 0.09	0.1	0.009
(mg DW cm^{-3})	Wheat‡	2.1 ± 0.7	0.09 ± 0.03	0.06 ± 0.01	0.03 ± 0.01	0.04 ± 0.02
Root length	Maize*	1.9 ± 0.3	0.9 ± 0.1	0.7 ± 0.1	0.7 ± 0.2	0.6 ± 0.2
(cm cm^{-3})	Wheat‡	2.1 ± 0.2	0.3 ± 0.05	0.2 ± 0.07	0.1	0.2

* data collected 24th October 2018; 171 days after sowing, $n = 4, 4, 3, 1, 1$.
‡ data collected between the 2-12th July 2019; 98–108 days after sowing, $n = 4, 4, 3, 2, 1$.

measured at 10, 20, and 30 cm depths (50 cm instead of 30 cm in 2018 soil temperature only). Where θ and temperature measurements at depth was absent for the calculation of the concentration gradient method (i.e. 30 or 50 cm), a gap filling method was used. By plotting the available data from the other depths and fitting different lines (linear, exponential, logarithmic or power), the best function was determined by the line that explained the most variation in the data (presented in Table S1, S2). The differences in the interpolation and extrapolation of the soil temperature data can be seen in Fig. S1. Normalised Difference Vegetation Index (NDVI) was measured weekly using a handheld GreenSeeker® crop sensor (Trimble Inc., Sunnyvale, CA, USA) held *ca.* 40 cm above the crop canopy. The crop height (base of plant to the tallest part) was also measured weekly, or more frequently, on 10 randomly selected plants per plot.

To characterise changes in inorganic N during the growing seasons, 5 g fresh soil samples ($n = 4$) were collected taken weekly during the growing seasons from augered (I.D. 2 cm) 0–5 cm depth. These were immediately extracted with 25 ml of 0.5 M K$_2$SO$_4$, shaken at 200 rev min^{-1} for 30 mins and centrifuged at 12,000 g for 5 mins before the supernatant was removed and analysed for NO$_3^-$-N and NH$_4^+$-N, as described above.

The maize and wheat fields were harvested on the 12th September

2018 and 2nd of September 2019, respectively. For maize, 4 plants per plot were randomly selected and oven dried (80 °C, 72 h). For wheat, 1 m strips of the 4 central rows from each plot where harvested and oven dried (80 °C, 72 h). On the 24th October 2018 and between the 2nd and 12th of July 2019, when the crops were fully established, soil cores (*ca.* 80 cm deep × 5 cm I.D.) were taken from each plot for root analysis using a percussion corer. Cores were cut into 10 cm sections (soil vol. *ca.* 196 cm^3) and washed to separate the roots from the soil. Roots were arranged on a plastic tray in water and scanned and analysed using the 2019 WinRhizo™ software (Regent Instruments Inc., Québec, Canada) to estimate total root length, before oven drying (70 °C, 24 h) to determine root biomass. The results are displayed in Table 1.

2.3. Greenhouse gas measurement systems

PVC pipes (3 cm diameter) of differing lengths (10, 20, 30 and 50 cm) were fitted with Suba-Seal® gas sampling ports at the top (Sigma-Aldrich ltd., Poole, UK). The final 3-cm region at the base of the pipe was perforated (0.8 mm diameter; *ca.* 20 holes) to allow gas ingress and the monitoring of GHGs at specific depths. The inside of this 3 cm section was lined with 1 mm nylon mesh to prevent soil entering the pipe and the base of the pipe was sealed with electrical tape (Fig. S2). In July 2019, the gas collecting pipes were fitted with plastic 2-way ($4 \times 1.2 \times 2.3$ cm) valves, where one end was sealed into a drilled hole in the headspace of the pipes and the other end had a 5 cm piece of silicon tubing attached to it (Fig. S2) for non-syringe gas sampling. In total, 8 pipes were made for each of the 4 depths ($n = 32$) and were inserted vertically to the desired depth by pushing them carefully into pre-cored holes (slightly smaller diameter). If the required depth was not reached by pushing alone, they were lightly tapped with a rubber mallet. These pipes were installed in mid-June 2018 when the field was under maize and sampled weekly until October 2018, after which they were carefully removed and maintained before re-inserting at the beginning of May 2019 for the wheat growing season. In 2019, 4 pipes of each depth were located in the High (150 kg ha^{-1}) and Medium (75 kg ha^{-1}) N fertilizer-applied blocks ($n = 4$).

The surface-atmosphere CO$_2$ flux was measured hourly by the chamber method (CM) with 12 *in situ* LI-COR LI-8100A automated soil CO$_2$ flux system with infrared gas analysis (LI-COR Biosciences, Inc., Lincoln, NE, USA) from 3rd of July to 7th of September 2018 and the 16th of May to the 30th of July and then from the 22nd of August until the 19th of September 2019. The gap in measurements in 2019 was due to equipment failure.

2.4. Gas sampling and analysis

Gas sampling occurred 1–3 times weekly from the 22nd of June to the 19th of September in 2018 and from the 22nd of May to the 19th of September in 2018 between 1000 and 1300 h. Using a gas-tight polypropylene syringe, air in the pipes was mixed by filling and emptying the syringe into the pipe 3 times before a *ca.* 25 ml gas sample was taken and over-filled (to prevent loss of sample during storage) into a pre-evacuated 20 ml glass vial (QUMA Elektronik & Analytik GmbH, Wuppertal, Germany). Before analysis, the samples were brought to ambient air pressure by inserting a needle into the vials and releasing the pressure. These were then analysed for CO$_2$, CH$_4$ and N$_2$O concentrations using a Perkin Elmer 580 Gas Chromatograph (GC), served with a Turbo Matrix 110 auto sampler (Perkin Elmer Inc., Waltham, MA). Gas samples passed through two Elite-Q mega bore columns via a split injector, with one connected to an electron capture detector (ECD) for N$_2$O determination, and the other to a flame ionisation detector (FID) for CO$_2$ and CH$_4$ determination.

2.5. CO$_2$ flux estimation

To estimate the fluxes of gases in the soil profile and at the soil

surface, the concentration gradient method (GM) was used (see review by Maier and Schack-Kirchner, 2014). The transport of gas through porous media in one dimension was approximated using Fick's first law:

$$F_z = -D_s \cdot \frac{dC}{dz} \quad (1)$$

where F is the gas flux (g CO_2 $m^{-2}h^{-1}$) at soil depth z (m), D_s is the effective gas diffusion coefficient of the gas in soil (m^2h^{-1}) and C is the concentration of the gas species (mg m^{-3}). As the direction of the concentration is decreasing, the given sign is negative (which can be ignored for the purposes of calculation). The concentration gradient (dC/dz) was calculated according to De Jong and Schappert (1972). The CO_2 concentration at depth 0 cm was taken as 409 ppm for 2018 and 412 ppm for 2019, according to the Mauna Loa Observatory data. The gas concentrations were converted from ppm to mg m^{-3} using Eq. (2), by multiplying the concentration by the molecular weight (M_w) of CO_2 (44.01 g mol^{-1}) and then dividing by the molar volume M_v (calculated by Avogadro's Law) of the gas:

$$C = \frac{M_w \cdot C'}{\left(\frac{R \cdot T}{P}\right)} \quad (2)$$

where C is the gas concentration in mg m^{-3}, C' is the gas concentration in ppmv, R is the universal gas constant (0.08206 L atm $K^{-1}mol^{-1}$), T is soil temperature (K) and P is pressure (atm).

The D_s was measured in February 2020 using a modified Currie chamber (Currie, 1960) and the DENitrification Incubation System (DENIS; Cárdenas et al., 2003) (Fig. S3). The methodology of the incubations is described in the Supplementary Information (S2). Briefly, SF_6 was used as a conservative tracer gas to determine the rate of diffusion through 104 cm^3 intact soil cores ($n = 6$) from the same field as in this study at depth intervals of 0–10 and 50–60 cm, at 0.3 and 0.5 air-filled porosities (ε). This resulted in a mean D_s of 0.0022 and 0.011 m^2h^{-1} in the 0.3 and 0.5 ε across all depths (the depths were not statistically different from each other). Field ε (cm^3 cm^{-3}) was estimated by subtracting the volumetric water content (θ; $cm^3 cm^{-3}$) from the total porosity of the soil as in Eq. (3), where B_d is dry bulk density (g cm^{-3}) and P_d is the particle density (assumed to be 2.65 g cm^{-3}).

$$\varepsilon = \left(1 - \frac{B_d}{P_d}\right) - \theta \quad (3)$$

Then, ε-related D_s was estimated from the relationship between mean D_s and ε. This was best explained at low ε ($<$50 %) by the power function: $D_s = 0.0907(\varepsilon)^{3.1848}$ ($R^2 = 0.99$). The effective diffusion coefficient for CO_2 was determined from the D_s of SF_6 by Eq. (4):

$$D_s = D'_s \cdot \frac{D_0}{D'_0} \quad (4)$$

where D'_s is the ε-related SF_6 diffusion coefficient, D'_0 is the diffusion coefficient of SF_6 in air (0.0335 m^2h^{-1}; Rudolph et al., 1996), and D_0 is the diffusion coefficient of CO_2 in air (0.0529 m^2h^{-1}). These were compared with the mean fluxes from the surface instruments between 1000 and 1300 h. The surface soil-atmosphere flux was estimated by extrapolating the fluxes from the 10 and 50 cm depths to the surface using Eq. (5) according to Hirano et al. (2003), where F_s is the surface flux and F_n (calculated using Eq. (1)) is the flux at depth z_n:

$$F_s = \frac{z_2 F_1 - z_1 F_2}{z_2 - z_1} \quad (5)$$

The cumulative flux was calculated by adding the fluxes from the first sampling date (where there were measurements from all gas dipwells and surface chambers) to the next time point fluxes and then the following fluxes until the end of the measurement period (i.e $F_1 = F_1$; $F_2 = F_1 + F_2$; $F_3 = F_1 + F_2 + F_3$). In 2019, due to surface chamber measurement failure, the cumulative flux was only calculated until the 24th July.

2.6. Gas consumption in laboratory mesocosms

In September 2019, *ca.* 50 g of soil was collected from each depth (10, 20, 30 and 50 cm) at 4 different sites within the same location as the maize and wheat field sites and sieved to 5 mm. Subsequently, 2 g replicates of field-moist soil were placed into 20 ml glass vials ($n = 4$) and mechanically sealed with a butyl septum (QUMA Elektronik & Analytik GmbH, Wuppertal, Germany) using a crimper. Two different gas mixes (gas chromatography standards) were injected into the vials: an ambient-approximate mix: 490 ppm of CO_2, 2 ppm of CH_4 and 310 ppb of N_2O; and a high-concentrated mix; 2800 ppm of CO_2, 32 ppm of CH_4 and 5500 ppb of N_2O. Both gas mixes were made up in 21 % O_2. This was done by flushing the vials with the gas mix for ca. 15 s at $>$100 ml min^{-1} with a needle while another needle allowed the purged headspace gas to escape. This same method was done with empty vials ($n = 4$), which confirmed the effectivity in replacing the headspace with the gas mix without loss of concentration. Three sets of identical vials containing four replicates from four soil depths at the two headspace concentrations were sampled at three different timepoints. After 24, 48 and 72 h incubating in the dark at room temperature (ca. 23 °C), 1 ml of gas was taken with a syringe from the headspaces of a set of vials and immediately filled into a new pre-evacuated vial. The new vials were then filled with 19 ml of N_2 gas (1:20 dilution) and analysed by gas chromatography (CO_2, CH_4 and N_2O), as described above. The gas fluxes were calculated on a dry weight basis according to the equations described by Comeau et al. (2018).

2.7. Data processing and statistical analysis

Zeros were removed from the CH_4 dataset due to being below the detection limit of the GC (limit of detection: ca. 1.42 ppm – see Supplementary Information, S1), resulting in the removal of 74 and 36 % of the maize and wheat CH_4 concentration data. In addition, the maize gas pipe GHG dataset from 2018 required selective removal of data, due to containing impossibly high values or zeros due to data far below or exceeding the concentrations of the analytical standards (see S1 for more detail). As the 2019 wheat dataset was of higher quality (see S1), this was used to inform and validate outlier removals in the 2018 maize dataset. Removing data that exceeded the single highest datapoints in 2019 and zeros, resulted in 19 and 9 % of the N_2O and CO_2 measurements being removed from the 2018 maize dataset, respectively.

All statistical data analysis was done on R (version 1.1.463; R Core Team, 2017). Before further analysis, as there were no differences between the concentrations at different depths with 2 rates of N fertilizer (two-way ANOVA) in the wheat growing season, GHG concentration gradient data were pooled (i.e. $n = 8$). One-way ANOVAs were used on the environmental measures with depth and Kruskal-Wallis rank sum tests were performed on the GHG concentration, GM flux means, soil temperature, and diffusivity data by depth, as they did not meet the assumptions for the equivalent parametric test following transformation (log, square root and cube). Mean GHG concentrations were compared between the maize and wheat growing seasons (equal-sized dataset of 10 weeks from 25th June to 5th September) by Welch's *t*-test. Two-way ANOVAs (Tukey's HSD) were performed on the GHG fluxes of the mesocosms by depth and headspace concentration. Trend lines were drawn for each wheat and maize GHG concentration gradient depth profile using Affinity Designer (Serif Europe ltd., Nottingham, UK).

3. Results

3.1. Environmental and crop conditions

The mean air temperature between the 1st May and 20th September in 2018 was 15.4 ± 0.06 °C with highest average daily temperatures of 20.6 on the 26th of June and lowest of 10 °C on the 8th of May. In the soil, average temperatures were 15, 12 and 8 % higher than in the air in

the 10, 30 and 50 cm depths (p <0.001), respectively. In 2019, the average air temperature was only 2 % lower than in 2018 (15.1 ± 0.3 °C), but experienced higher maximum and minimum daily average temperatures of 25.2 °C on 27th June and a 7.5 °C on 3rd May (Fig. 1a), respectively. Similar to 2018, mean soil temperatures in 2019 were 13, 12 and 11 % higher than in the air than at 10, 20 and 30 cm (p <0.001), respectively.

The total precipitation for the 1st May − 20th September period was 208 mm in 2018 and 381 mm in 2019 (Fig. 1b). The wettest months in this period in 2018 were September > August > July > May > June, where the entirety of June had only 2 mm of rainfall. In stark comparison, June was 54-fold wetter and the wettest month in the same period

in 2019 with 115 mm followed by August > July > September > May. Interestingly, in 2018 soil water content increased and in 2019 decreased with depth. Mean volumetric water content (θ) was the same in 2019 in the 10 and 20 cm depths (0.26 cm^3 cm^{-3}) and slightly lower at 30 cm (0.24 cm^3 cm^{-3}). In 2018, between the 6th June and the 20th September mean θ was 0.16, 0.17 and 0.18 cm^3 cm^{-3} in the 10, 20 and 50 cm depths, respectively. With the lower water content in the soil profile throughout 2018, the mean estimated diffusivity of SF$_6$ (low solubility; 0.0017 m^{2}h^{-1}) was 1.7-fold higher in all depths, compared to 2019 (p <0.001; Fig. 1c). Mean diffusivity decreased with depth similarly in both years (p <0.001), with 5–7 and 79 % lower diffusivity at 20 and 30 cm respectively compared to the diffusivity of the soil at 10 cm.
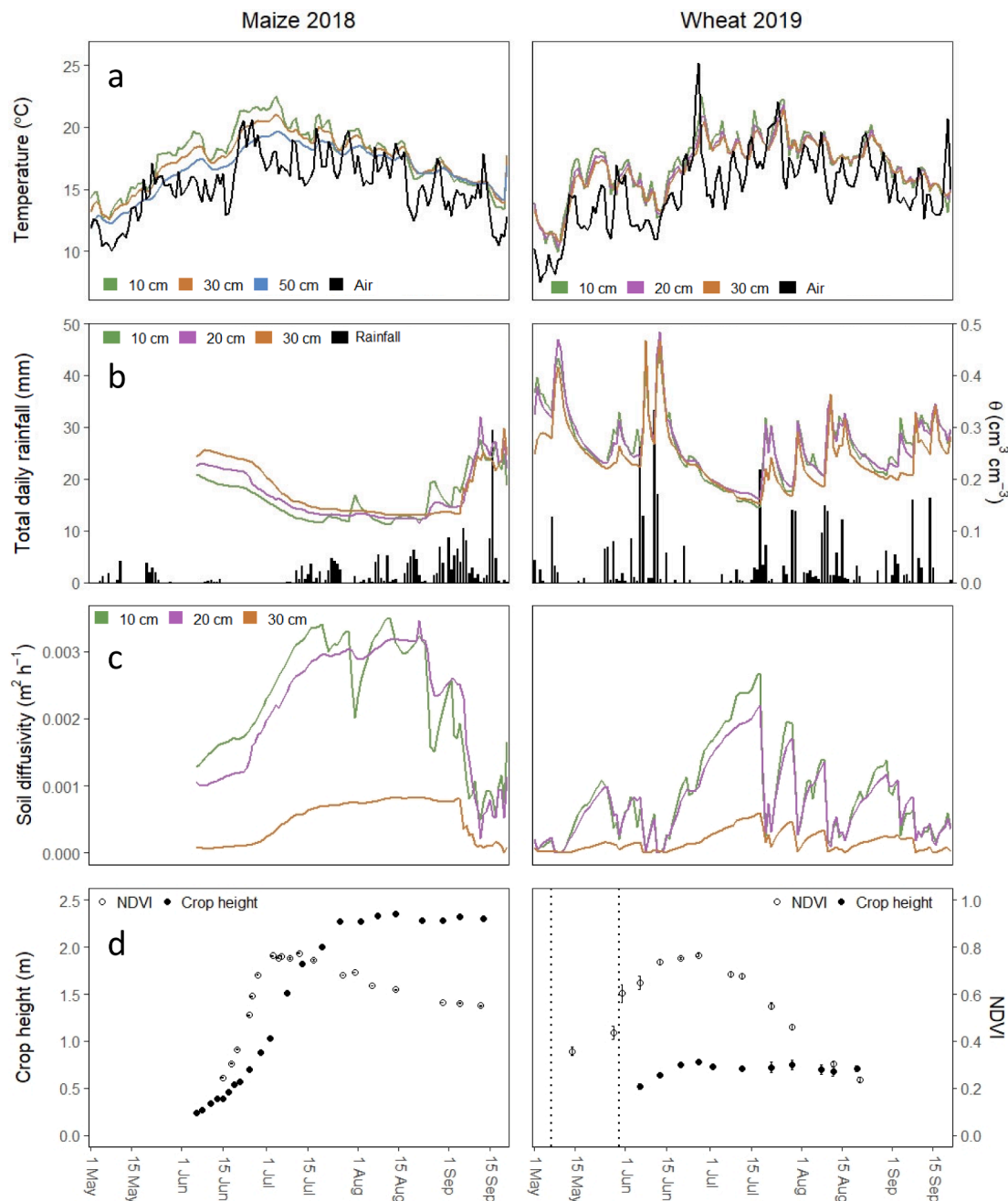
Fig. 1. Daily average a) air and soil temperature; b) total daily precipitation and average volumetric water content (θ); c) estimated diffusivity of SF$_6$ through the soil of different depths; and d) mean (±SEM) crop height ($n = 10$) and NDVI ($n = 4$) during the 2018 and 2019 growing seasons (1st May – 20th Sep). Colours reflect different measurement depths. The vertical dotted lines are the dates when ammonium nitrate fertilizer was applied in 2019, where 40 kg ha^{-1} was applied on the 7th May and 110 kg ha^{-1} on the 30th May.

In 2018, the highest mean NDVI was measured as 0.77 ± 0.01 on the 12th July, while the highest plant height of 2.4 m ± 0.02 was measured >1 month later on the 14th August. The week of the 27th June was the warmest week of the season and when both the highest mean NDVI (0.77 ± 0.01) and crop heights (0.78 m ± 0.01) were measured. The largest increase in NDVI in 2019 was following N fertilizer addition on the 31st May (Fig. 1d).

3.2. GHG concentrations at depth

Across both growing seasons, the concentrations of CO_2 and N_2O in the gas pipes were consistently higher than atmospheric concentrations and increased with soil depth, while the opposite trend was observed with CH_4 concentrations (Fig. 2). The mean CO_2 concentrations were greater under wheat compared to maize at all depths (Fig. 2a; $p < 0.001$). Under maize and wheat, CO_2 concentrations increased with soil depth ($p < 0.001$; $p < 0.001$, respectively). There was no difference in mean N_2O concentrations between the maize and wheat growing seasons (Fig. 2b; $p = 0.11$). Both the maize and wheat N_2O concentrations were greater with depth ($p < 0.001$). The mean CH_4 concentrations across the soil profile were not different between the maize and wheat growing seasons (Fig. 2c; $p = 0.23$). The decrease in CH_4 concentration with soil depth was not significant under maize ($p = 0.14$), but CH_4 concentrations decreased with soil depth in the wheat season ($p < 0.001$).

3.3. Measured and estimated CO_2 fluxes with soil depth

The concentration of CO_2 (Fig. 3a) in the gas collection pipes increased with greater soil depth ($p < 0.001$) and differed across growing season ($p < 0.001$) under both the maize and wheat.

The extrapolation of the GM estimates of the soil depth fluxes produced a good estimate of the soil surface flux in the wheat 2019 season (Fig. 3b & c), demonstrated by only 6 % difference between the measured surface flux (0.52 ± 0.05 g CO_2 m^{-2}h^{-1}) and the GM surface flux ($p = 0.72$). In the maize season, the mean measured surface flux (0.54 ± 0.08 g CO_2 m^{-2}h^{-1}) was 28 % higher than the GM estimated surface flux ($p = 0.004$; Fig. 3b & c) in 2018. When comparing the GM estimated CO_2 fluxes with those that were measured, the maize linear fit only explained 10 % of the variation in the data with a line slope below 1 (of the 1:1 line) of 0.62, while 46 % of the variation in the data was explained by the 1.02 slope of the wheat season linear correlation (Fig. 4).

In the 2018 maize growing season (Fig. 3b), the overall mean estimated CO_2 flux was 6, 17, 17 and 54-fold lower in the 0–10, 10–20, 20–30 and 30–50 cm depths than measured at the soil surface (0.52 ± 0.07 g CO_2 m^{-2}h^{-1}), respectively. This corresponds to a contribution of 21, 9, 11 and 0.05 % to the estimated cumulative surface flux (5.79 g CO_2 m^{-2}) from the 0–10, 10–20, 20–30 and 30–50 cm depths (Fig. 3c), respectively, suggesting that these depths contributed ca. 41 % to the surface flux. The CO_2 fluxes in the 2019 wheat growing season were 4, 23, 105 and 1365-fold lower in the 0–10, 10–20, 20–30 and 30–50 cm depths than measured at the surface (0.54 ± 0.08 g CO_2 m^{-2}h^{-1}), respectively. The contribution to the estimated cumulative surface flux (7.37 g CO_2 m^{-2}) of the 0–10, 10–20, 20–30 and 30–50 cm depths was therefore lower with 20, 4, 1 and 0.08 %, respectively, or a total of 26 % (Fig. 3c).

3.4. Production and consumption of GHGs in laboratory mesocosms

In the vials where an ambient gas mix was added, the fluxes of all gases showed an increase in gas production from the soil during the 3 d incubation (Fig. 5). However, following the addition of the highly concentrated gas mix a decrease in all gas fluxes was observed, apart from CO_2 in the shallow depths. The mean fluxes of the ambient treatments were significantly greater than those of the highly concentrated headspace treatments in all gases ($p < 0.001$). The gas concentrations in
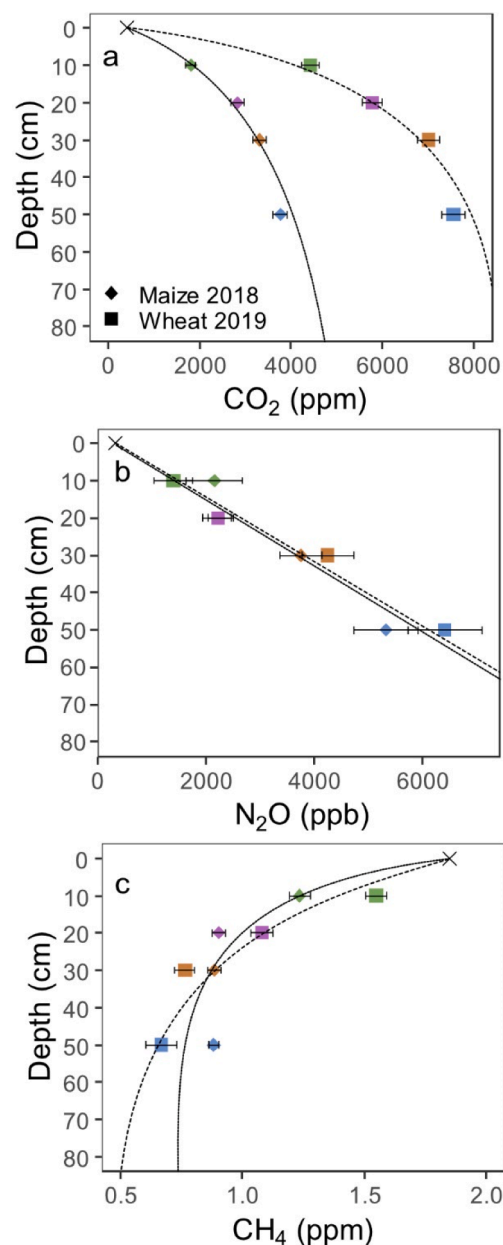
Fig. 2. Depth profiles of mean ($\pm$SEM) gas concentrations of a) CO_2; b) N_2O; and c) CH_4 from weekly sampling of gas collectors installed at different soil depths ($n = 8$) in a field under maize in 2018 (22 Jun 2018 – 19 Sep 2018; $N = 644$) and wheat in 2019 (22 May 2019 – 5 Sep 2019; $N = 533$). Colours reflect different sampling depths. Solid and dotted lines represent the maize and wheat, respectively. The 'X' at 0 cm depth represents the approximate ambient levels of the respective gases (CO_2, 420 ppm; N_2O, 330 ppb; CH_4, 1.85 ppm, respectively). The curves were forced to intercept the x-axis (0 cm) at the aforementioned concentrations.

the no-soil blanks remained stable over the 72 h period, confirming that there were no leaks.

Both soil depth and headspace gas concentration had a significant effect on the fluxes of the GHGs, but the added headspace concentration had the stronger effect (Fig. 5). The flux of CO_2 production in ambient concentrated CO_2 headspace was significantly higher at soil depth ≥ 20 cm ($p < 0.001$). Similarly, in the highly concentrated headspace, the production flux was higher in the ≥ 10 cm soil depths ($p < 0.001$; Fig. 5), whereas the 30 and 50 cm depths were sinks of CO_2. As CH_4 was produced in the ambient headspace, the flux was greater than in the high concentration headspace ($p < 0.001$) but was not different with depth (p
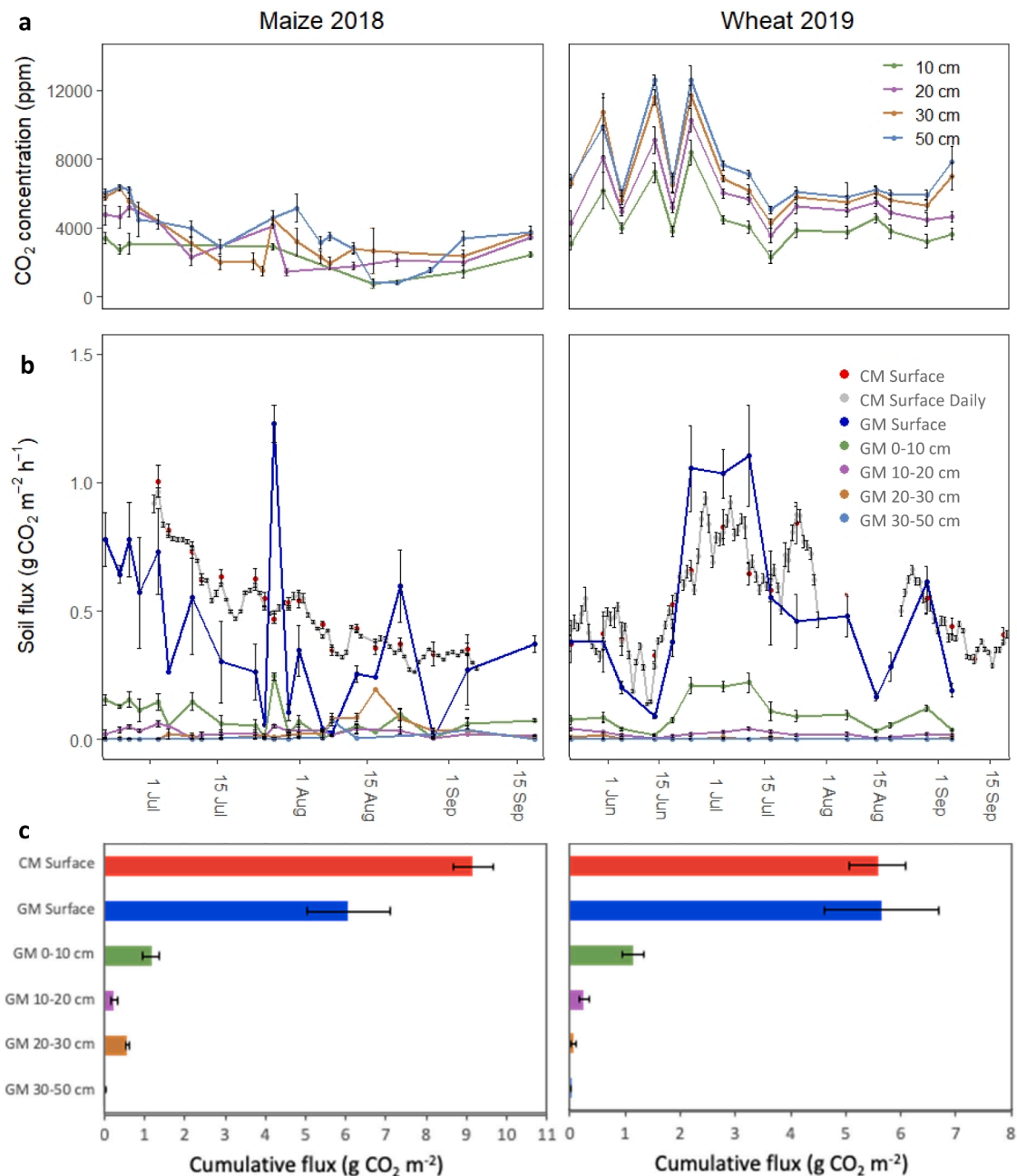
Fig. 3. The a) mean (±SEM) CO_2 concentrations from the gas collectors installed at different depths ($n = 8$); b) measured (CM) and estimated (GM) CO_2 fluxes (mean ± SEM) at different depths in the soil profile ($n = 8$); and c) cumulative CO_2 flux of the mean measured and estimated fluxes from different depths. 'CM Surface Daily' is the mean 24 h surface CO_2 flux, while 'CM Surface' is the mean surface flux between 1000 and 1300 h - the same sampling times and days as for the gas collector sampling. The cumulative fluxes in c) include periods of comparative data (3rd Jul – 5th Sep in 2018; and 22nd May – 24th July in 2019).

= 0.4). In contrast, in the highly concentrated headspace, the CH_4 flux was depth dependent ($p < 0.001$). The flux in the 10 and 20 cm depths was only 6 % different, but 27–57 % lower than the 30 and 50 cm fluxes, respectively. Finally, more N_2O was produced in the ambient headspace incubation ($p < 0.001$) than in the high concentration headspace, but the flux of N_2O was not different between depths in the ambient gas treatment ($p = 0.06$). In the high concentration headspace, 22–34 % more N_2O was consumed at 10 and 20 cm compared to 30 and 50 cm depths ($p < 0.001$).

4. Discussion

4.1. Soil CO_2 concentrations, fluxes and GM estimations

The convex-shaped depth profiles of CO_2 concentrations are consistent with other studies in tropical forest (Davidson et al., 2004) and semi-arid arable (Wang et al., 2013; Wang et al., 2018) systems. The CO_2 concentrations were significantly higher in all depths in the wheat growing season compared to those under maize (Fig. 3a). While this is as hypothesised, it is unlikely due to crop-related root respiration as the rooting density was highest under maize (Table 1). Therefore, it is more likely explained by environmental factors affecting biotic and abiotic processes, driven by the differences in climatic conditions experienced
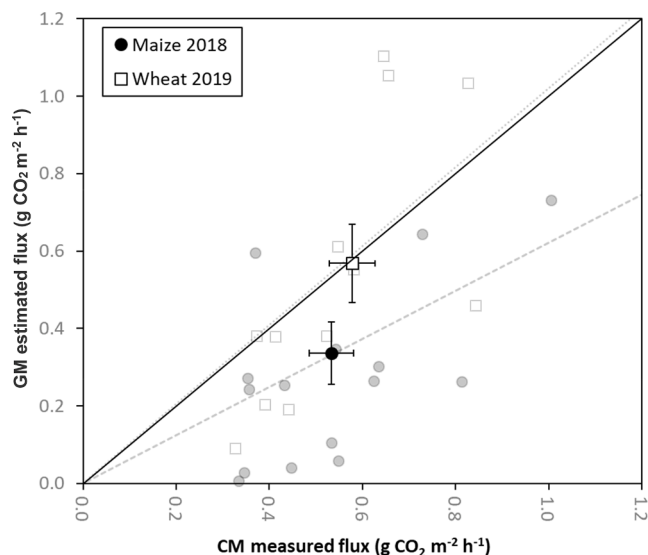
Fig. 4. The mean surface measured (CM) versus estimated (GM) CO_2 flux ($\pm$SEM) in a field under maize ($n = 12$) or wheat ($n = 16$) production. The grey symbols points represent the raw data while the transparent dashed line is the linear correlation for maize ($y = 0.62x$, $R^2 = 0.10$) and the transparent dotted line is the corresponding correlation for wheat ($y = 1.02x$, $R^2 = 0.46$). The trend lines are forced through 0 at the y-intercept. The solid line is the 1:1 line ($y = x$).

in 2018 versus those in 2019. 2018 was an exceptionally dry year compared to long term rainfall data (Turner et al., 2021). Compared to 2019, the 2018 growing season had 84 % less precipitation and the soil water content was a third lower, resulting in a 170 % increase in soil diffusivity (Fig. 1). This would suggest that the differences in CO_2 are primarily driven by these physical rather than biotic differences in the soil, as CO_2 retention in the soil profile is primarily influenced by the diffusivity of the soil (Risk et al., 2002). Therefore, in the dry 2018 season, a reduction in the soils capacity to retain CO_2 means the potential accumulation of CO_2 in the soil is limited. In addition, the formation of large cracks and macropores in the field due to the drought will have created heterogeneity in soil diffusion and a more rapid escape of CO_2 from depth (Deurer et al., 2009). This is also supported by observations of Kochiieru et al. (2018) who demonstrated the importance of macropores in moderating soil surface CO_2 fluxes, albeit for topsoils.

The drier conditions under maize may also have affected the seal of the gas collection pipes with the surrounding soil, resulting in dilution of the samples with less concentrated atmospheric air which diffuses into the soil (as the pipes are vertically installed; Fig. S2). However, if this made a significant contribution, the CH_4 and N_2O concentrations may be expected to also be lower in the 2018 growing season which they were not, meaning either atmospheric dilution of the samples is unlikely to have been the main reason for the lower concentrations; or, if there was dilution, other factors prevented the concentrations to differ in the CH_4 and N_2O concentration profiles (i.e. higher production, lower diffusion).

While the CO_2 fluxes of the wheat growing season were estimated reliably by the GM, as hypothesised, the maize growing season fluxes were underestimated (Fig. 4). However, in both cases, higher agreement between the measured and estimated fluxes was expected. The reason for the low agreement is likely due to many factors, as the GM relies on many input variables for the extrapolation of estimated soil fluxes to the soil surface. However, physical chamber-based effects also influence the resultant surface flux in the CM (Maier and Schack-Kirchner, 2014). Therefore, reliably determining which method is more representative of the true *in situ* flux is a challenge (Yu et al., 2013). Due to the high spatial and temporal heterogeneity of soil fluxes, we attribute the lower agreement to the GM measurements not being taken at the exact same time or location as the CM measurements. The particularly poor performance of the GM in the maize year suggests that the GM presented is unreliable in estimating fluxes under drought conditions experienced in 2018. However, differences in pore and soil structure driven by drought were unaccounted for in the measured D_s, which has strong influence over the GM results. *In situ* measurement of the D_s alongside the gas profile measurements would give the best GM estimations (Maier and Schack-Kirchner, 2014) and may have prevented underestimation.

The large overestimation of the GM fluxes, most notably on the 27th July 2018 (Fig. 4b), is likely due to an increase in CO_2 concentrations measured at shallower soil depths (i.e. 20 and 30 cm; Fig. 4a) causing the GM to extrapolate the surface flux inaccurately. High CO_2 concentrations close to the surface can occur following precipitation after a sustained period of warm dry weather causing a bidirectional concentration gradient (Pingintha et al., 2010). This pulse of CO_2 production is called the 'Birch' effect (Barnard et al., 2020) and considering the drought conditions and increase in precipitation from mid-July (Fig. 1), this could explain the flux overestimations. This scenario represents a potential weakness in the accuracy of the GM that needs to be considered.

In this study, the 0–10, 10–20, 20–30 and 30–50 cm depths in the
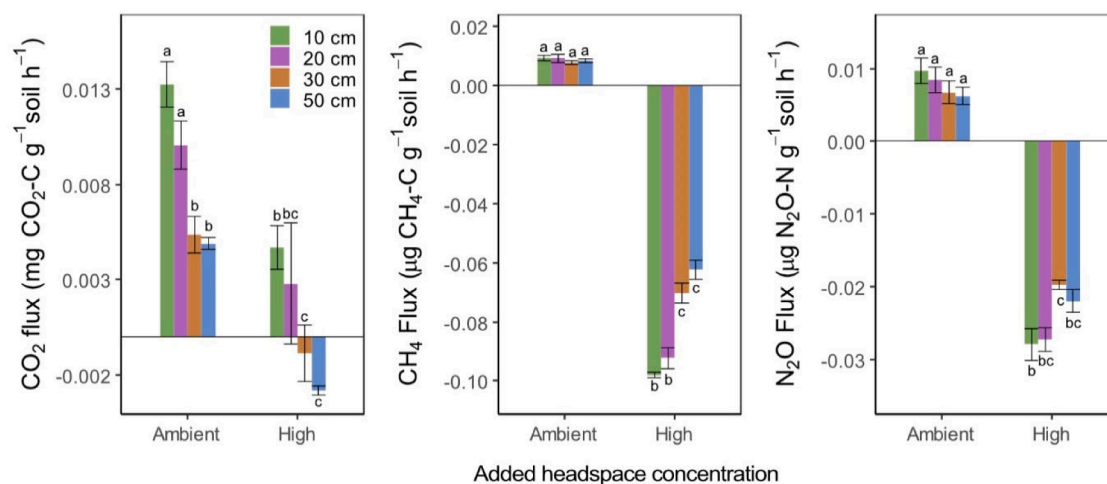
Fig. 5. Net fluxes (means $\pm$ SEM) of CO_2, CH_4, and N_2O of destructively sampled ($n = 4$) soil of different depths incubated for 72 h with added headspace gas concentrations: Ambient (490 ppm CO_2; 2 ppm CH_4; 310 ppb of N_2O) and High (2800 ppm CO_2; 32 ppm CH_4; 5500 ppb N_2O). Different letters indicate significant differences between the gas concentrations of the soil depths and headspace concentrations for each GHG at $p < 0.05$ (Tukey). Positive values indicate production and negative values indicate consumption.

2019 growing season were estimated to contribute 20, 4, 1 and 0.08 % to the surface flux, respectively. As the 2018 estimated fluxes are underestimated (Fig. 4), their contributions to the surface flux are likely to be greater than the 21, 9, 11 and 0.05 % estimated for the 0–10, 10–20, 20–30 and 30–50 cm depths, respectively. The decrease in CO_2 production with depth was consistent with the lower root distribution of wheat and maize down the soil profile (Table 1). The 2019 flux contributions correspond well with both Xiao et al. (2015) and Wang et al. (2018) who estimated the 0–5 cm layer to contribute 70–90 % and only around 2 % below a soil depth of 15 cm. The 2018 growing season had a greater contribution from the 10–20 and 20–30 cm depths, which could be due to fine root mortality at depth and subsequent decomposition (Davidson et al., 2004). The higher water content at depth throughout most of the 2018 growing season (Fig. 1) supports the idea that decomposition conditions were relatively enhanced deeper in the soil compared to soil near the surface.

The laboratory-based ambient headspace incubation demonstrated that CO_2 was microbially produced across the 72 h incubation period and was significantly higher in the shallower soil depth (Fig. 5). The fluxes from this incubation fall within the range of mean CO_2 production estimated by the GM in the field both years at the same depths (i.e. 0.38 – 82 mg CO_2 $m^{-2}h^{-1}$). The flux of CO_2 consumption differed with depth in the highly concentrated headspace incubation (Fig. 5). While a decrease in CO_2 production with depth is well established and supported by data from this study (Figs. 3 and 5), the biotic consumption of CO_2 remains relatively understudied. Microbial dark CO_2 fixation is a process reported to decrease with depth in temperate soil (Akinyede et al., 2020), increase with greater CO_2 concentration (Spohn et al., 2020) and be optimal close to 25 °C (Nel and Cramer, 2019). The fluxes we measured agree with the range measured (0.2 – 4.8 mg CO_2 $m^{-2}h^{-1}$) in a short (30 mins) incubation of agricultural surface soil by Shimmel (1987) and at the lower end of the range (2.8 – 36.5 mg CO_2 $m^{-2}h^{-1}$) of longer (21 d) temperate field and forest topsoil incubations (Santruckova et al., 2005). The net fluxes measured in this incubation will be a balance between the production and fixation of CO_2. The net negative fluxes in the high CO_2 concentration headspace in the 30 and 50 cm depths (Fig. 5) suggests the fixation flux was greater than the production flux. While the higher than *in situ* temperatures in the incubation would have enhanced both fluxes (Nel and Cramer, 2019; Risk et al., 2002), the 'high' CO_2 concentration added as headspace (ca. 2800 ppm) is lower than the average CO_2 concentrations at all depths under normal growing conditions (2019; Fig. 2). Using higher CO_2 headspace concentrations would likely have increased the fixation flux but may have been cancelled out by using lower *in situ* temperatures. In addition, as CH_4 oxidation produces CO_2, this could have accounted for a small percentage of the net CO_2 flux of the shallow soil in the high headspace gas concentration treatment. Without disentangling the origins and processes of the CO_2 measured, it is not possible to confirm whether dark CO_2 fixation is depth dependent in this arable soil. We suggest measuring dark fixation via ^{14}C-labelled CO_2 as this method is much more sensitive and predominantly measures unidirectional influx over short labelling periods.

4.2. Soil N₂O concentrations and fluxes

The lack of differences between N_2O concentrations in the soil with different fertilising regimes (Fig. 2) suggests that 1) either the majority of the N_2O in the soil profile was not fertiliser derived, despite substantial available inorganic N in the topsoil (Fig. S4) and that NO_3^- content relates well with N_2O concentrations; or 2) the balance between spatially and temporally heterogenous N_2O production and consumption processes are responsible for the observed N_2O concentrations, which are influenced by many physical, chemical and biological factors. N_2O concentrations increased with depth in a linear trend and the mean values were not different between the growing seasons (Fig. 3), which is in contrast to our hypothesis that they would differ with growing season.

This is consistent with the N_2O concentration profiles across 2 maize growing seasons reported by Wang et al. (2018). However, considering the differences in soil temperature, water content and soil diffusivity between 2018 and 2019 in this study (Fig. 1), a difference in N_2O concentrations would be expected due to their effect on key N_2O production and consumption processes (i.e. nitrification and denitrification). Nitrification, although considered less important than denitrification in generating N_2O in most agricultural soils, can be the dominant N_2O producing process (e.g. North China Plain; Zhang et al., 2016) and can produce N_2O in tandem with denitrification (Bateman and Baggs, 2005). However, generally, a high soil water content means consumption and production of N_2O will be greater (ca. $\geq$ 60 % WFPS; Bateman and Baggs, 2005). While higher soil water content under wheat means greater gas retention, it also means slower diffusion and longer residence time in the soil resulting in a higher potential for N_2O denitrification to N_2, which is greatest at high moisture contents (Clough et al., 2005; Neftel et al., 2007). In addition, C released from roots is expected to stimulate microbial respiration causing localised O_2 depletion, which can further drive N_2O consumption. While wheat root density and length were 60 and 40 % lower than in the maize at 0–50 cm (Table 1), respectively, wheat roots release a greater amount of exudates per gram of dry root weight (Vančura et al., 1977). Finally, NO_3^- concentrations were greater in the 2018 year (Fig. S4) which can lead to higher N_2O concentrations in the profile (Wang et al., 2013). Therefore, we conclude that the N_2O concentrations in the wheat growing seasons are not greater than those in the maize due to lower production resulting from low NO_3^- concentrations and possibly also due to higher fluxes of N_2O consumption.

Despite the fluxes of N_2O production not statistically differing with soil depth in the mesocosm incubation (Fig. 5), the trend in means clearly show a decrease in production with depth. The data does demonstrate significantly greater N_2O consumption in shallower soil (10 and 20 cm; Fig. 5). Despite the evidence of depth dependent N_2O consumption, we concede that using only 2 g of soil from one point in time and incubated at higher temperatures at ambient O_2 concentration is unlikely to capture the full extent of consumption and production fluxes observed *in situ*. Especially as N_2O production, consumption and movement may be more complex than that of CO_2 and CH_4, partly due to N_2O consumption fluxes having greater spatial and temporal variability in soil (Mosier et al., 1998; Wang et al., 2018).

4.3. Soil CH₄ concentrations and fluxes

Despite no expected difference between the overall CH_4 concentrations with crop, they did decrease with depth (Fig. 2) which is consistent with other studies (Wang et al., 2013; Wang et al., 2018). As anaerobic conditions are required for methanogenesis, production of CH_4 is likely to be very low within the soil profile and while anaerobic (micro)sites may occur and produce CH_4 in the soil profile, this can be almost completely oxidised in aerated soil zones (Le Mer and Roger, 2001). The ambient atmospheric concentration of CH_4 is consistently higher than in the profile, suggesting that oxidation of CH_4 by methanotrophs occurs throughout the soil profile (Wang et al., 2013; Wang et al., 2018). This is supported by the results shown in Fig. 5, where CH_4 is oxidised at all soil depths included. Therefore, the lack of a difference between the maize and wheat CH_4 concentrations was more likely due to the similar soil microbial community rather than differences in crop root structure.

As expected, consumption of CH_4 was depth dependent with greater consumption occurring in shallower soil. This agrees with the results of Wang et al. (2018), who found CH_4 consumption to decrease with soil depth. As temperature is not a major controlling factor in CH_4 oxidation in the non-extreme environment in this study (Le Mer and Roger, 2001), the fluxes measured at a higher temperatures in the incubation are likely reasonably representative of those *in situ*.

5. Conclusions

Here we provide GHG concentration profiles and further proof of concept of the GM in a lowland arable context with low resolution (weekly) data over an extended period (2 y). A reasonable GM extrapolation of the surface CO_2 flux from soil gas collectors under average growing conditions was achieved despite low temporal resolution. Drought conditions caused significant GM underestimation of the surface flux, due to the greater soil diffusivity associated with lower soil moisture unaccounted for by the D_s. This likely also caused the CO_2 concentration depth profile to be different between growing seasons. The N_2O concentration profile was only marginally affected by soil inorganic N concentration. Finally, we provide evidence of depth dependent CH_4 oxidation, N_2O consumption and possibly CO_2 fixation. With the study of a singular maize-wheat rotation across different environmental conditions, more year replicates are needed to make more meaningful comparisons between these crops and their interaction with the soil and the GM. The results of this study improve our understanding of the opportunities and limitations of the GM and of GHG dynamics in the soil profile of a temperate arable system.

Declaration of Competing Interest

The authors declare that they have no known competing financial interests or personal relationships that could have appeared to influence the work reported in this paper.

Data availability

Data will be made available on request.

Acknowledgements

Appendix A. Supplementary data

Supplementary data to this article can be found online at https://doi.org/10.1016/j.geoderma.2022.116310.

References

Akinyede, R., Taubert, M., Schrumpf, M., Trumbore, S., Küsel, K., 2020. Rates of dark CO_2 fixation are driven by microbial biomass in a temperate forest soil. Soil Biol. Biochem. 150, 107950 https://doi.org/10.1016/j.soilbio.2020.107950.

Barnard, R.L., Blazewicz, S.J., Firestone, M.K., 2020. Rewetting of soil: Revisiting the origin of soil CO_2 emissions. Soil Biol. Biochem. 147, 107819 https://doi.org/10.1016/j.soilbio.2020.107819.

Bartelt-Ryser, J., Joshi, J., Schmid, B., Brandl, H., Balser, T., 2005. Soil feedbacks of plant diversity on soil microbial communities and subsequent plant growth. Perspect. Plant Ecol. Evol. Syst. 7, 27–49. https://doi.org/10.1016/j.ppees.2004.11.002.

Bateman, E.J., Baggs, E.M., 2005. Contributions of nitrification and denitrification to N2O emissions from soils at different water-filled pore space. Biol. Fertil. Soils 41, 379–388. https://doi.org/10.1007/s00374-005-0858-3.

Boon, A., Robinson, J.S., Chadwick, D.R., Cardenas, L.M., 2014. Effect of cattle urine addition on the surface emissions and subsurface concentrations of greenhouse gases in a UK peat grassland. Agric. Ecosyst. Environ. 186, 23–32. https://doi.org/10.1016/j.agee.2014.01.008.

Button, E.S., Pett-Ridge, J., Murphy, D.V., Kuzyakov, Y., Chadwick, D.R., Jones, D.L., 2022. Deep-C storage: Biological, chemical and physical strategies to enhance carbon stocks in agricultural subsoils. Soil Biol. Biochem. 170, 108697.

Cárdenas, L.M., Hawkins, J.M.B., Chadwick, D., Scholefield, D., 2003. Biogenic gas emissions from soils measured using a new automated laboratory incubation system. Soil Biol. Biochem. 35, 867–870. https://doi.org/10.1016/S0038-0717(03)00092-0.

Chapuis-Lardy, L., Wrage, N., Metay, A., Chotte, J.L., Bernoux, M., 2007. Soils, a sink for N2O? A review. Glob. Chang. Biol. 13, 1–17. https://doi.org/10.1111/j.1365-2486.2006.01280.x.

Clark, M., Jarvis, S., Maltby, E., 2001. An improved technique for measuring concentration of soil gases at depth in situ. Commun. Soil Sci. Plant Anal. 32, 369–377. https://doi.org/10.1081/CSS-100103013.

Clough, T.J., Sherlock, R.R., Rolston, D.E., 2005. A review of the movement and fate of N2O in the subsoil. Nutr. Cycl. Agroecosystems 72, 3–11. https://doi.org/10.1007/s10705-004-7349-z.

Comeau, L.P., Lai, D.Y.F., Cui, J.J., Hartill, J., 2018. Soil heterotrophic respiration assessment using minimally disturbed soil microcosm cores. MethodsX 5, 834–840. https://doi.org/10.1016/j.mex.2018.07.014.

Currie, J.A., 1960. Gaseous diffusion in porous media Part 1. - A non-steady state method. Br. J. Appl. Phys. 11, 314–317. https://doi.org/10.1088/0508-3443/11/8/302.

Davidson, E.A., Ishida, F.Y., Nepstad, D.C., 2004. Effects of an experimental drought on soil emissions of carbon dioxide, methane, nitrous oxide, and nitric oxide in a moist tropical forest. Glob. Chang. Biol. 10, 718–730. https://doi.org/10.1111/j.1529-8817.2003.00762.x.

de Sosa, L.L., Glanville, H.C., Marshall, M.R., Williams, A.P., Abadie, M., Clark, I.M., Blaud, A., Jones, D.L., 2018. Spatial zoning of microbial functions and plant-soil nitrogen dynamics across a riparian area in an extensively grazed livestock system. Soil Biol. Biochem. 120, 153–164. https://doi.org/10.1016/j.soilbio.2018.02.004.

De-Polli, H., Costantini, A., Romanik, R., Pimentel, M.S., 2007. Chloroform fumigation-extraction labile C pool (microbial biomass C "plus") shows high correlation to microbial biomass C in Argentinian and Brazilian soils. Cienc. del Suelo 25, 15–22.

Deurer, M., Grinev, D., Young, I., Clothier, B.E., Müller, K., 2009. The impact of soil carbon management on soil macropore structure: A comparison of two apple orchard systems in New Zealand. Eur. J. Soil Sci. 60, 945–955. https://doi.org/10.1111/j.1365-2389.2009.01164.x.

Dossa, G.G.O., Paudel, E., Wang, H., Cao, K., Schaefer, D., Harrison, R.D., 2015. Correct calculation of CO_2 efflux using a closed-chamber linked to a non-dispersive infrared gas analyzer. Methods Ecol. Evol. 6, 1435–1442. https://doi.org/10.1111/2041-210X.12451.

Fiedler, S.R., Buczko, U., Jurasinski, G., Glatzel, S., 2015. Soil respiration after tillage under different fertiliser treatments - implications for modelling and balancing. Soil Tillage Res. 150, 30–42. https://doi.org/10.1016/j.still.2014.12.015.

Hirano, T., Kim, H., Tanaka, Y., 2003. Long-term half-hourly measurement of soil CO_2 concentration and soil respiration in a temperate deciduous forest. J. Geophys. Res. Atmos. 108 https://doi.org/10.1029/2003JD003766.

Johnston, A.E., Poulton, P.R., Coleman, K., 2009. Soil Organic Matter. Its Importance in Sustainable Agriculture and Carbon Dioxide Fluxes. Adv. Agron. 101, 1–57. https://doi.org/10.1016/S0065-2113(08)00801-8.

Jong, E.D., Schappert, H.J., 1972. Calculation of soil respiration and activity from CO_2 profiles in the soil. Soil Sci. 113, 328–333. https://doi.org/10.1097/00010694-197205000-00006.

Kochiieru, M., Lamorski, K., Feiza, V., Feizienė, D., Volungevičius, J., 2018. The effect of soil macroporosity, temperature and water content on CO_2 efflux in the soils of different genesis and land management. Zemdirbyste 105, 291–298. https://doi.org/10.13080/z-a.2018.105.037.

Kusa, K., Sawamoto, T., Hu, R., Hatano, R., 2008. Comparison of the closed-chamber and gas concentration gradient methods for measurement of CO_2 and N_2O fluxes in two upland field soils. Soil Sci. Plant Nutr. 54, 777–785. https://doi.org/10.1111/j.1747-0765.2008.00292.x.

Le Mer, J., Roger, P., 2001. Production, oxidation, emission and consumption of methane by soils: A review. Eur. J. Soil Biol. 37, 25–50. https://doi.org/10.1016/S1164-5563(01)01067-6.

Li, Z., Kelliher, F.M., 2005. Determining nitrous oxide emissions from subsurface measurements in grazed pasture: A field trial of alternative technology. Aust. J. Soil Res. 43, 677–687. https://doi.org/10.1071/SR04106.

Maier, M., Schack-Kirchner, H., 2014. Using the gradient method to determine soil gas flux: A review. Agric. For. Meteorol. 192–193, 78–95. https://doi.org/10.1016/j.agrformet.2014.03.006.

Miranda, K.M., Espey, M.G., Wink, D.A., 2001. A rapid, simple spectrophotometric method for simultaneous detection of nitrate and nitrite. Nitric Oxide - Biol. Chem. 5, 62–71. https://doi.org/10.1006/niox.2000.0319.

Mosier, A., Kroeze, C., Nevison, C., Oenema, O., Seitzinger, S., van Cleemput, O., 1998. Closing the global N_2O budget: nitrous oxide emissions through the agricultural nitrogen cycle. Nutr. Cycl. Agroecosystems 52, 225–248.

Mulvaney, R.L.-M. of soil analysis, 1996. Nitrogen—inorganic forms. SSSA, Madison 3, pp 1123–1184.

Neftel, A., Flechard, C., Ammann, C., Conen, F., Emmenegger, L., Zeyer, K., 2007. Experimental assessment of N_2O background fluxes in grassland systems. Tellus Ser. B Chem. Phys. Meteorol. 59, 470–482. https://doi.org/10.1111/j.1600-0889.2007.00273.x.

Nel, J.A., Cramer, M.D., 2019. Soil microbial anaplerotic CO2 fixation in temperate soils. Geoderma 335, 170–178. https://doi.org/10.1016/j.geoderma.2018.08.014.

Pingintha, N., Leclerc, M.Y., Beasley, J.P., Zhang, G., Senthong, C., 2010. Assessment of the soil CO_2 gradient method for soil CO_2 efflux measurements: Comparison of six models in the calculation of the relative gas diffusion coefficient. Tellus Ser. B Chem. Phys. Meteorol. 62, 47–58. https://doi.org/10.1111/j.1600-0889.2009.00445.x.

R Core Team, 2017. A language and environment for statistical computing. R.

Risk, D., Kellman, L., Beltrami, H., 2002. Carbon dioxide in soil profiles: Production and temperature dependence. Geophys. Res. Lett. 29, 1–4. https://doi.org/10.1029/2001GL014002.

Rudolph, J., Rothfuss, F., Conrad, R., 1996. Flux between soil and atmosphere, vertical concentration profiles in soil, and turnover of nitric oxide: 1. Measurements on a model soil core. J. Atmos. Chem. 23, 253–273. https://doi.org/10.1007/BF00055156.

Santruckova, H., Bird, M.I., Elhottová, D., Novák, J., Picek, T., Šimek, M., Tykva, R., 2005. Heterotrophic fixation of CO_2 in soil. Microb. Ecol. 49, 218–225. https://doi.org/10.1007/s00248-004-0164-x.

Shimmel, S.M., 1987. Dark fixation of carbon dioxide in an agricultural soil. Soil Sci. 144 (1), 20–23.

Spohn, M., Müller, K., Höschen, C., Mueller, C.W., Marhan, S., 2020. Dark microbial CO_2 fixation in temperate forest soils increases with CO_2 concentration. Glob. Chang. Biol. 26, 1926–1935. https://doi.org/10.1111/gcb.14937.

Staff, S.S., 2014. Keys to Soil Taxonomy, 12th ed. USDA. Resources Conservation Services, Washington, DC.

Sumner, M.E., Miller, W.P., 1996. Cation Exchange Capacity and Exchange Coefficients, Methods of. ed. https://doi.org/https://doi.org/10.2136/sssabookser5.3.c40.

Turner, S., Barker, L.J., Hannaford, J., Muchan, K., Parry, S., Sefton, C., 2021. The 2018/2019 drought in the UK: a hydrological appraisal. Weather 76, 248–253. https://doi.org/10.1002/wea.4003.

Vance, E.D., Brookes, P.C., Jenkinson, D.S., 1987. An Extraction Method for Measuring Soil Microbial Biomass. Soil Biol. Biochem. 19, 703–707. https://doi.org/10.1016/0038-0717(87)90052-6.

Vančura, V., Přikryl, Z., Kalachová, L., Wurst, M., 1977. Some Quantitative Aspects of Root Exudation. Soil Org. Components Ecosyst. 25, 381–386.

Wang, Y.Y., Hu, C.S., Ming, H., Zhang, Y.M., Li, X.X., Dong, W.X., Oenema, O., 2013. Concentration profiles of CH_4, CO_2 and N_2O in soils of a wheat–maize rotation ecosystem in North China Plain, measured weekly over a whole year. Agric. Ecosyst. Environ. 164, 260–272.

Wang, Y., Li, X., Dong, W., Wu, D., Hu, C., Zhang, Y., Luo, Y., 2018. Depth-dependent greenhouse gas production and consumption in an upland cropping system in northern China. Geoderma 319, 100–112. https://doi.org/10.1016/j.geoderma.2018.01.001.

Xiao, X., Kuang, X., Sauer, T.J., Heitman, J.L., Horton, R., 2015. Bare Soil Carbon Dioxide Fluxes with Time and Depth Determined by High-Resolution Gradient-Based Measurements and Surface Chambers. Soil Sci. Soc. Am. J. 79 (4), 1073–1083.

Yu, L., Wang, H., Wang, G., Song, W., Huang, Y., Li, S.G., Liang, N., Tang, Y., He, J.S., 2013. A comparison of methane emission measurements using eddy covariance and manual and automated chamber-based techniques in Tibetan Plateau alpine wetland. Environ. Pollution 181, 81–90.

Zhang, Y., Mu, Y., Zhou, Y., Tian, D., Liu, J., Zhang, C., 2016. NO and N_2O emissions from agricultural fields in the North China Plain: Origination and mitigation. Sci. Total Environ. 551–552, 197–204. https://doi.org/10.1016/j.scitotenv.2016.01.209.